Title

Impacts of weather conditions modified by urban expansion on surface ozone: Comparison between the Pearl River Delta and Yangtze River Delta regions

Journal

Advances in Atmospheric Sciences, 26(5)

ISSN

0256-1530

Authors

Wang, Xuemei
Chen, Fei
Wu, Zhiyong
et al.

Publication Date

2009-09-01

DOI

10.1007/s00376-009-8001-2

ADVANCES IN ATMOSPHERIC SCIENCES, VOL. 26, NO. 5, 2009, 962–972

Impacts of Weather Conditions Modified by Urban Expansion on Surface Ozone: Comparison between the Pearl River Delta and Yangtze River Delta Regions

WANG Xuemei*[1] (王雪梅), CHEN Fei[2] (陈 飞), WU Zhiyong[1] (吴志勇), ZHANG Meigen[3] (张美根), Mukul TEWARI[2], Alex GUENTHER[2], and Christine WIEDINMYER[2]

[1]*School of Environmental Science and Engineering, Sun Yat-sen University, Guangzhou* 510275

[2]*National Center for Atmospheric Research, Boulder, CO* 80305*, USA*

[3]*Institute of Atmospheric Physics, Chinese Academy of Sciences, Beijing* 100029

(Received 25 August 2008; revised 19 December 2008)

ABSTRACT

In this paper, the online weather research and forecasting and chemistry (WRF-Chem) model is used to explore the impacts of urban expansion on regional weather conditions and its implication on surface ozone concentrations over the Pearl River Delta(PRD) and Yangtze River Delta(YRD) regions. Two scenarios of urban maps are used in the WRF-Chem to represent the early 1990s (pre-urbanization) and the current urban distribution in the PRD and the YRD. Month-long simulation results using the above land-use scenarios for March 2001 show that urbanization increases both the day- and night-time 2-m temperatures by about 0.6°C and 1.4°C, respectively. Daytime reduction in the wind speed by about 3.0 m s^{-1} is larger than that for the nighttime (0.5 to 2 m s^{-1}). The daytime increase in the PBL height (> 200 m) is also larger than the nighttime (50–100 m). The meteorological conditions modified by urbanization lead to detectable ozone-concentration changes in the PRD and the YRD. Urbanization increases the nighttime surface-ozone concentrations by about 4.7%–8.5% and by about 2.9%–4.2% for the daytime. In addition to modifying individual meteorological variables, urbanization also enhances the convergence zones, especially in the PRD. More importantly, urbanization has different effects on the surface ozone for the PRD and the YRD, presumably due to their urbanization characteristics and geographical locations. Even though the PRD has a smaller increase in the surface temperature than the YRD, it has (a) weaker surface wind speed, (b) smaller increase in PBL heights, and (c) stronger convergence zones. The latter three factors outweighed the temperature increase and resulted in a larger ozone enhancement in the PRD than the YRD.

Key words: urbanization, Pearl River Delta (PRD), Yangtze River Delta (YRD), surface ozone concentrations, WRF-Chem

Citation: Wang, X. M., F. Chen, Z. Y. Wu, M. G. Zhang, M. Tewari, A. Guenther, and C. Wiedinmyer, 2009: Impacts of weather conditions modified by urban expansion on surface ozone: Comparison between the Pearl River Delta and Yangtze River Delta regions. *Adv. Atmos. Sci*, **26**(5), 962–972, doi: 10.1007/s00376-009-8001-2.

1. Introduction

Changes in land use and land cover (LULC) alter the exchange of energy, momentum, moisture, and other trace gases within the vegetation-soil-atmosphere continuum, subsequently affecting the global and regional climate (Charney et al., 1977; Chase et al., 1996; Foley et al., 2005), and hence impacting the dispersion of pollutants and air quality. The Pearl River Delta (PRD) and the Yangtze River Delta (YRD) regions are the most two advanced economic districts in China, which have experienced remarkable economic development and urbanization in the past two decades. The GDP for these two districts is about 29.5% of the total Chinese GDP in 2006. Urban areas account for 60% in the total land cover in

*Corresponding author: WANG Xuemei, eeswxm@mail.sysu.edu.cn

PRD, which is two times higher than the Chinese national average, and for about 45% in YRD. The expanded urban areas in these two districts were generally converted from farm lands. The PRD region, an area of about 41700 km^2, located in the southern part of the Guangdong Province, includes mega-cities such as Hong Kong, Guangzhou, Shenzhen, and seven other mid-size cities. The YRD region with area of 109600 km^2 is located in east-central China, which includes the Jiangsu Province, Shanghai, the Zhejiang Province, and a part of the Jiangxi Province and the Anhui Province. There are 16 cities in YRD including the mega-cities of Shanghai, Nanjing, Suzhou, Wuxi, and Hangzhou. However the urban spatial sprawls in PRD and YRD are different. For instance, in PRD, cities are connected with each other and form a city cluster (see Fig. 1d); in YRD, the urban expansion and clustering of surrounding towns and counties are located in centralized cities, like Shanghai and along the Ningbo-Shanghai-Hangzhou transport passageway Yao and Chen (1998).

The fast urbanization is significantly modifying local and regional meteorological conditions. Climatologic data indicates that the mean winter temperature of southern China, including PRD, increased by approximately 0.0326°C yr^{-1} for the past 37 years (Liang and Wu, 1999). In YRD, three urban heat island centers also showed a temperature increase: Shanghai with up to 0.025°C yr^{-1} (the highest value in this region), a second heat island in the center to the southeast of Nantong city with an increase of 0.020°C yr^{-1}, and along the Suzhou-Wuxi-Changzhou line neighboring the Taihu Lake with an increase of 0.015°C yr^{-1}–0.020°C yr^{-1} (He and Zhuang, 2005). In recent years, severe air pollution episodes with high ozone and poor visibility occur in alarming frequency throughout PRD (Lee and Sequeira, 2001; Wang et al., 2001), Chan et al. (2003) also reported high levels of air pollutants on China's east coast over Lin'an. Recent studies on the impacts of urbanization on local weather and air quality mainly focused on Hong Kong and PRD. Lo et al. (2006), using an atmospheric model and a three-dimensional particle trajectory model, pointed out that urbanization in the PRD can modify regional land-sea-breeze circulations and potentially enhance the pollutant trapping, and therefore may contribute to the overall poor air quality in the region. Lin et al. (2007) used the MM5 model to simulate the impact of urban expansion on monthly climate in the PRD region. Wang et al. (2007) used a regional atmospheric chemistry model to study the effects of urbanization on surface ozone concentrations in the PRD. These investigations were based on case studies, and the impacts of urbanization on air quality in YRD region have not been quantified.

The PRD and YRD are both located in the coastal regions, and both have experienced remarkable economic development and urbanization in the past two decades. Continuing urbanization in these two regions puts a significant strain on natural resources and impacts the air quality and regional climate; it is, hence, necessary to understand and compare the effects of urbanization on air quality between these two heavily urbanized delta regions, which may provide insightful input to policy makers for regional sustainable development. Therefore, the main objective of our study is to use the weather research and forecasting with online chemistry (WRF-Chem) model to conduct month-long simulations to examine the degree to which urbanization-induced weather conditions impact surface ozone in highly-urbanized regions located in slightly different climate regions: the PRD and YRD. Month-long simulations are necessary to investigate how ozone distributions respond to changes in atmospheric conditions due to urbanization under different synoptic weather regimes (rather than looking at one single weather event). Here, we primarily focus on the analysis of ozone modification (because ozone is the most important oxidant and indicator of photochemical smog) to changing meteorological conditions and do not consider the impact of a change in emissions on ozone concentrations. Measurements of tropospheric O_3 over East Asia and the western Pacific in Japan, Taiwan, and Hong Kong show a maximum concentration in the spring (Logan, 1985; Oltmans et al., 1992; Harris et al., 1998; Chan et al., 1998; Langford, 1999). A climatological tropospheric O_3 map derived from satellite data (Fishman and Brackett, 1997) over China also shows a springtime maxima. Therefore, we chose March 2001 for this study because it comprises several high-pollution episodes, and air-quality data is available for evaluating the model simulations.

2. Methodology

2.1 *Description of the WRF-Chem model*

The WRF-Chem is used to simulate the impacts of urban expansion on weather conditions and surface ozone concentrations in March 2001. Details of the WRF-Chem model can be found in Grell et al. (2005) and at http://ruc.fsl.noaa.gov/wrf/WG11/. This numerical model system is "online" in the sense that all processes affecting the gas phase and the aerosol species are calculated concurrently with the meteorological dynamics. It has been successfully applied for regional air quality studies (Fast et al., 2006).

Different physics and chemistry options in the WRF-Chem can be used. In this study, we used the physical parameterizations including the NCEP-5 class microphysics (Hong et al., 1998), a new Kain-Fritsch convective parameterization (Kain, 2004), Dudhia shortwave radiation (Dudhia, 1989), RRTM longwave radiation Mlawer et al. (1997), the Yonsei University (YSU) planetary boundary layer (PBL) scheme (Noh et al., 2003), and the Noah land surface scheme (Chen and Dudhia, 2001). The Noah LSM provides surface sensible and latent heat fluxes, and surface skin temperatures as the lower boundary conditions to WRF. To represent the thermal and dynamic effects of urban areas, the single-layer urban canopy model (UCM) of Kusaka et al. (2001) and Kusaka and Kimura (2004) was coupled to Noah in the WRF-Chem model. The basic function of a UCM is to take urban geometry into account in its surface energy budgets and wind shear calculations (Miao and Chen, 2008) and to calculate the surface fluxes from man-made surfaces and include (Jiang et al., 2008): (1) 2-D street canyons that are parameterized to represent the effects of urban geometry on urban canyon heat distribution; (2) shadowing from buildings and reflection of radiation in the canopy layer; (3) the canyon orientation and diurnal cycle of the solar azimuth angle; (4) man-made surface consisting of eight canyons with different orientations; (5) Inoue's model for canopy flows (Inoue, 1963); (6) the multi-layer heat equation for the roof, wall, and road interior temperatures; and (7) a very thin bucket model for evaporation and runoff from road surfaces. The CBM-Z gas-phase photochemical mechanism (Zaveri and Peters, 1999) and the model for simulating aerosol interactions and chemistry (MOSAIC) (Fast et al., 2006) were used in this study. The Fast-J radiation scheme (Wild et al., 2000) was chosen to calculate photolysis rates from the predicted ozone, aerosols, and cloud profiles.

2.2 *Anthropogenic emission and biogenic emission*

The anthropogenic emission distribution used in this analysis is based on the estimates of Streets et al. (2003). Estimates of emissions from individual sectors (i.e., industry, power, domestic, transportation, and shipping) are included in the analysis. We improved the emission rates of SO_2, NO_x, and PM_{10} through the use of local, detailed information (Wang et al., 2005). Measurements obtained in the TRACE-P(transport and chemical evolution over the Pacific) experiment during February and April, 2001 are used in conjunction with regional modeling analysis to evaluate emission estimates for Asia (Carmichael et al., 2003a,b). It was found that the emission inventories are of sufficient quality to support preliminary studies of ozone production. Biogenic emissions are calculated online using the BEIS (biogenic emissions inventory system) model (Guenther et al., 1995). As our main objective is to explore the influences of urban-induced changes in meteorological conditions on air quality, we used the same surface biogenic and industrial emission rates (reflecting today's situation) for different land-use scenarios. The impacts of the emission rate changes will be investigated in future studies.

2.3 *Land-use data used in this study*

Two land-use scenarios are used in the WRF-Chem model for the PRD and the YRD regions in this study to explore the effects of urban expansion on weather and air pollution. The WRF-Chem model is configured for the current study with a horizontal grid spacing of 12 km and grid point dimensions of 171×171. The location of the domain is shown in Fig. 1a, which covers the southeastern part of China, centered at 27.2°N and 116.0°E with 24 vertical layers up to 100 hPa. The default land-use data used in the WRF-Chem model is based on the 1992–1993 1-km Advanced Very High Resolution Radiometer (AVHRR) data (see Fig. 1b and Fig. 1c), which, to a large degree, reflects the distribution of cities (mainly Shanghai, Nanjing, Guangzhou, and Hong Kong) in the late 1980s. By contrast, an updated land-use scheme based on the 2004 1-km Moderate Resolution Imaging Spectroradiometer (MODIS) (Friedl et al., 2002) data is used to refer to today's distributions of cities (see Fig. 1d and Fig. 1e). The latter demonstrates the rapidly urbanized areas centered in Guangzhou, Foshan, Dongguan, and Shenzhen in the PRD and Shanghai, Hangzhou, Nanjing, Suzhou, and Wuxi in the YRD. The 1-km MODIS data are aggregated onto a 12-km domain using the same approach in the WRF to aggregate the 1-km USGS land-use data.

The WRF-Chem/UCM simulation started from 0000 UTC 01 March 2001 and ended at 2300 UTC 30 March 2001. Therefore, two month-long WRF-Chem simulations are conducted with identical WRF-Chem physics packages, initial, and boundary conditions, and the only exception is that one simulation used the 1993 default land-use data (referred to as the Pre-urban simulation hereafter) and the other used the 2004 MODIS land-use data (referred to as the Urban simulation hereafter).

3. Model validation

3.1 *Verification for chemical species*

Measurement data from the Hok Tsui monitoring site are used to evaluate the chemical mechanisms in the WRF-Chem. The Hok Tsui site (22.2°N, 114.3°E) established by the Hong Kong (HK) Polytechnic Uni-

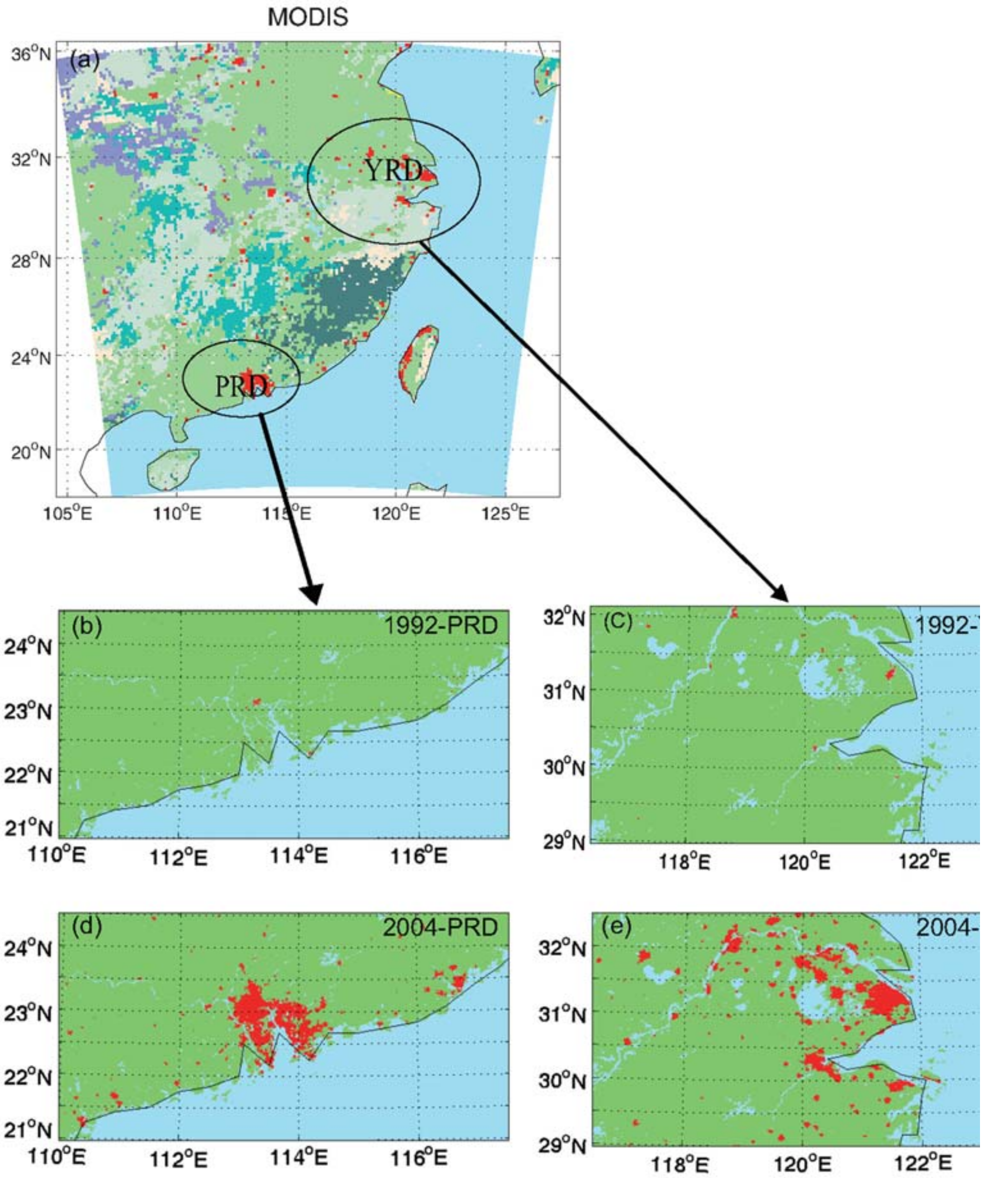

Fig. 1. The modeling domain and land-use data sets used for the WRF-Chem simulations: (a) WRF-Chem domain with 12-km grid spacing, (b) 1992–1993 USGS data of PRD, (c) 1992–1993 USGS data of YRD, (d) 2004 MODIS data of PRD, (e) 2004 MODIS data of YRD. The only change between (b) and (d), (c) and (e) is the urban areas marked in red.

versity, is located on the southeastern tip of Hong Kong Island. A detailed description of the site and its surroundings is given by Wang et al. (2001). Briefly, the site was selected to reflect the atmospheric transport and conversion processes in a relatively clean area of Hong Kong. This site is located ∼20 km away from the city center and downwind of the city under the prevailing east-northeast flows in the spring. The measured trace gases are NO_y, CO, SO_2, O_3, and NO at Hok Tsui. Here, NO_y at Hok Tusi includes NO, NO_2, NO_z (PAN, HONO, HNO_3, N_2O_5 and organic nitrates).

As discussed by Wang et al. (2003b), the rural HK site can be influenced by urban plumes, as indicated by sharp rises in the time series of the hourly averaged mixing ratios of NO_y, CO, SO_2, O_3 (Fig. 2). March is a transitional period between the winter and summer monsoons. The Siberian high system and the Pacific high system come and go in this region (Bey et al., 2001; Wang et al., 2003a), which results in large day-to-day variations in the trace gas levels. Several peaks during this month are shown in Fig. 2.

Two main chemical mechanisms were chosen for comparison tests under the same physical parameter-

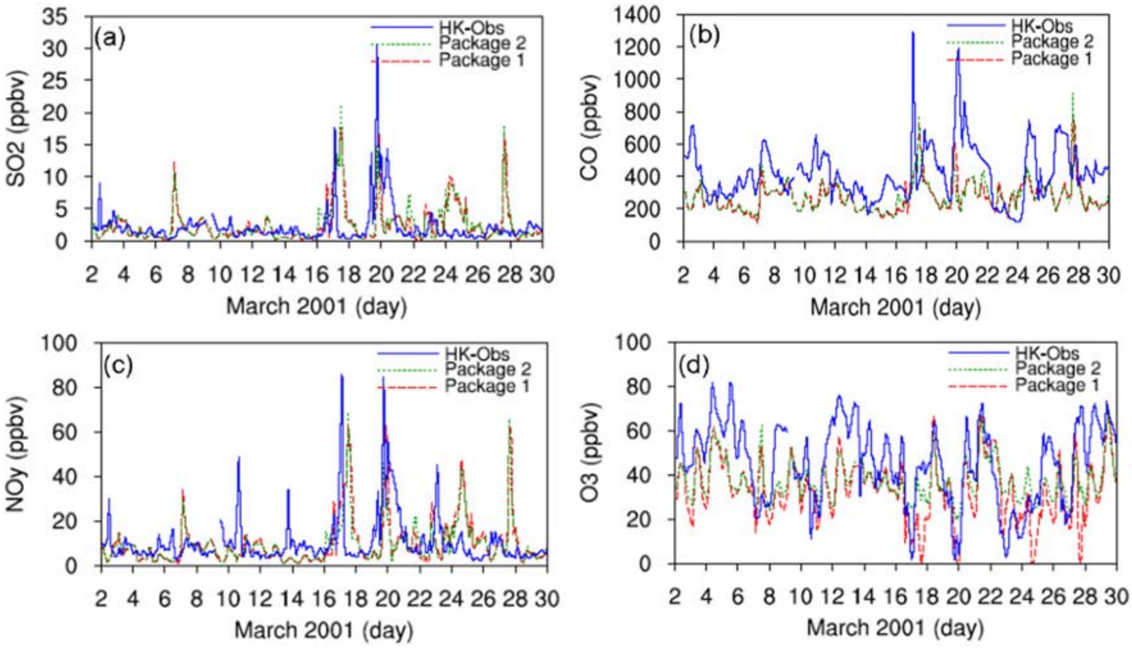

Fig. 2. Time series of the various pollutants measured at the HK site for March 2001 as compared to the WRF-Chem simulations: (a) SO_2, (b) CO, (c) NO_y, (d) O_3. Solid lines: observations; red dotted lines: WRF-Chem simulation with Package 1; green dotted lines: WRF-Chem simulation with Package 2.

izations. Package 1 is CBM-Z and MOSAIC for the gas phase and aerosol species. Package 2 is RADM2 (Regional Acid Deposition Model version 2) for the gas phase chemical reaction, and MADE (Modal Aerosol Dynamics Model for Europe)-SORGAM (Secondary Organic Aerosol Model) mechanisms for the aerosol species. Figure 2 shows the time series of the various pollutants measured at the HK measurement site for March 2001 as compared to the WRF-CHEM simulations. The simulations are able to capture many of the observed features. For example, the increase in CO, SO_2, and NO_y during 18–22 March is well captured in the simulations. The model clearly shows a distinct tendency to under predict O_3 concentrations during the daytime. Several possible reasons are available to explain such a low bias in O_3 during the daytime in the WRF-Chem model. One inaccuracy is the emission inventory. The VOC and CO emission rates are under estimate in this study (Streets et al., 2003), which is shown in Fig. 2b. Several studies indicate that PRD is a VOC limited area, and underestimating VOC in the emission inventory may have caused a lower O_3 formation in the daytime. Comparing these two chemical mechanisms, we found that the results from package 1 can better represent a nighttime ozone titration that agrees with the observations. We found that package 2 tends to over predict the OH concentration at low NO_x levels at night, which can lead to a reduction of the destruction of O_3 production. So in this study, we choose package 1 as a chemical mechanism for the other sensitive studies.

3.2 *Verification of meteorological variables*

The WRF-Chem simulated meteorological conditions are evaluated against surface measurements from 19 weather stations located within our modeling domain. The verification statistics of 2-m temperature, 10-m wind speed, and 2-m relative humidity for the

Table 1. Comparison of meteorological variables of the WRF-Chem simulation and the observations (N_stn: number of stations, Mean: mean value, Obs: observation, Sim: simulation, MAE: mean absolute error, RMSE: root mean square error, HR: hit rate).

Meteorological variables	N_stn	Mean		Bias	MAE	RMSE	HR
		Obs	Sim				
2-m temperature (°C)	22	18.3	19.0	0.7	1.8	2.3	0.63
2-m RH (%)	22	75.5	70.2	−5.3	10.5	13.5	0.86
10-m wind speed ($m\,s^{-1}$)	19	3.2	4.5	1.3	2.0	2.6	0.30

entire time period are shown in Table 1. Hit rate (HR) (Schlünzen and Katzfey, 2003), the root mean square error (RMSE), and other statistics are calculated. In statistics, the bias, the mean absolute error (MAE), and the root mean square error (RMSE) are frequently-used measures of the differences between model simulations and the observations, and are defined as:

$$\text{Bias} = \frac{1}{n}\sum_{i=1}^{n}(S_i - O_i) ,$$

$$\text{MAE} = \frac{1}{n}\sum_{i=1}^{n}|S_i - O_i| ,$$

$$\text{RMSE} = \sqrt{\frac{1}{n}\sum_{i=1}^{n}(S_i - O_i)^2} ,$$

respectively, where S_i is the simulation and O_i is the observation. Besides those above, another measure, the HR (hit rate) is introduced here. The hit rate means that out of the total number of stations, how many are within a certain threshold. In this paper, the criteria for the hit rate calculation are for a model-observation agreement within 2°C for the 2-m temperatures, 10% for the 2-m relative humidity, and 1 m s^{-1} for the 10-m wind speed. The hit rate is a reliable overall measure for describing the model performance, because it is able to consider the measurement uncertainty, which is difficult to consider in the bias, MAE or RMSE.

In Table 1, the simulated 2-m temperature is higher (0.7°C) than the observed data, while the simulated 2-m RH is a little lower (5.3%). Therefore, the WRF/Noah/UCM modeling system appears to produce a "warmer" and "drier" simulation. The hit rates of the 2-m temperature and RH are 0.63 and 0.86, respectively, reflecting good agreements between the observations and the simulations. The simulated wind speed is about 1.3 m s^{-1} higher than the observed. As expected from the relatively strict criteria (1 m s^{-1}), the HR of the wind speed (0.30) is the lowest among all the variables. In the study of Miao et al. (2009), a 24-h WRF/Noah/UCM simulation in relation to the Beijing area on 18–19 August 2005, was conducted. According to the same criteria for the 2-m temperature (2°C) and the 10-m wind speed (1 m s^{-1}), the hit rate calculation and the 2 g kg^{-1} for the 2-m specific humidity, the HR of the 2-m temperature, the 2-m specific humidity, and the 10-m wind speed are 0.78, 0.61, and 0.75, respectively. The HR of the temperature and humidity in Table 1 are close to those above, while the hit rate of the wind speed is much lower than that in Miao et al. (2009). Nevertheless, the mean observed 10-m wind speed is only 0.98 m s^{-1} in that case while 3.2 m s^{-1} in this. So the criteria for the wind speed (1 m s^{-1}) hit rate calculation becomes really strict in this case. In summary, these statistics suggest that the WRF/Noah/UCM modeling system generally captures the synoptic systems and the regional weather fairly well.

4. Results and analysis

4.1 *Regional weather-condition changes induced by urban expansion*

In recent years, many efforts have been made to estimate the weather condition changes due to urbanization. The results revealed that air temperature, wind field, humidity, and the height of the atmosphere boundary layer induced by the land-use change (Grossman-Clarke et al., 2005; Liu et al., 2006; Lo et al., 2006; Civerolo et al., 2000; Jiang et al., 2008) can affect the production and distribution of air pollutants (Taha et al., 1998; Civerolo et al., 2007; Wang et al., 2007). In this study, we focused on three parameters: 2-m air temperature, PBL heights, and 10-m wind speed because of their significant roles in the formation and evolution of surface ozone concentrations (Ordonez et al., 2005).

The difference of the monthly mean 2-m air temperatures between urban and pre-urban simulations shows that urbanization increases both the daytime and nighttime 2-m temperatures (Fig. 3) in the PRD and the YRD. However, the temperature increase for the daytime is smaller than that for the nighttime. The maximum difference between the simulations with pre-urban and urban is about 0.6°C in the daytime

Table 2. Relative differences of the variables between the urban and pre-urban simulations in the urban areas. For a given variable X, the ratio is defined as $\frac{X_{\text{Urban}} - X_{\text{Pre-urban}}}{X_{\text{Pre-urban}}} \times 100$.

	Variables							
	T2		10-m wind		PBL Height		O_3	
Locations	day	night	day	night	day	night	day	night
PRD	1.0	3.7	−40.3	−38.2	6.3	5.9	4.2	8.5
YRD	2.5	20.5	−35.5	−19.4	9.7	35.3	2.9	4.7

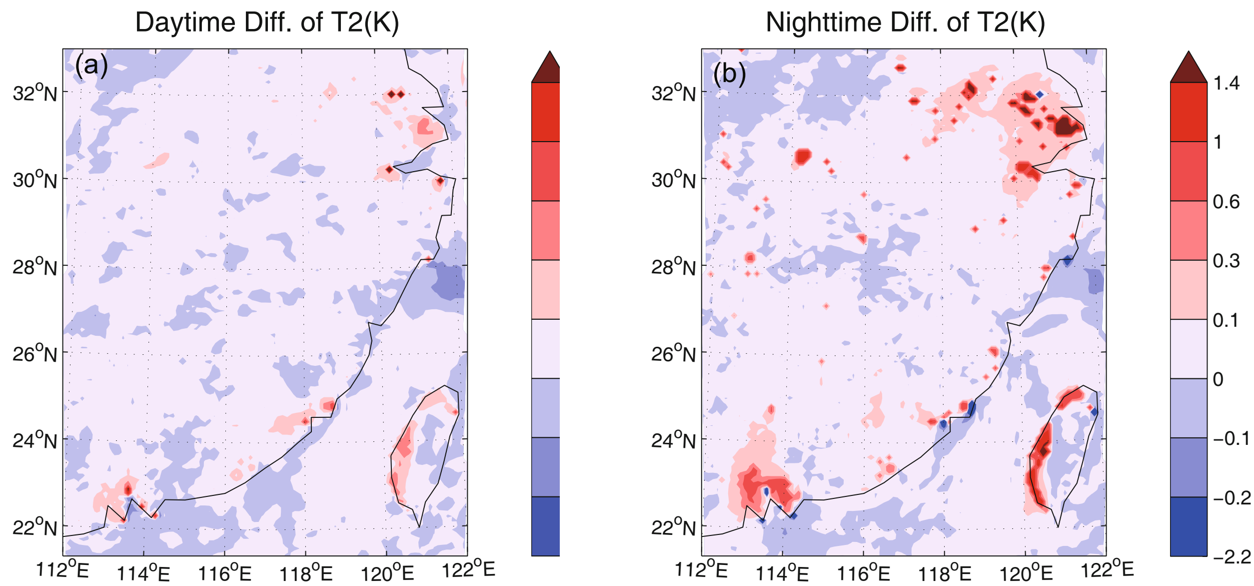

Fig. 3. Differences of the 2-m temperatures (K) between the urban and pre-urban simulations. (a) Monthly average for the daytime and (b) monthly average for the nighttime.

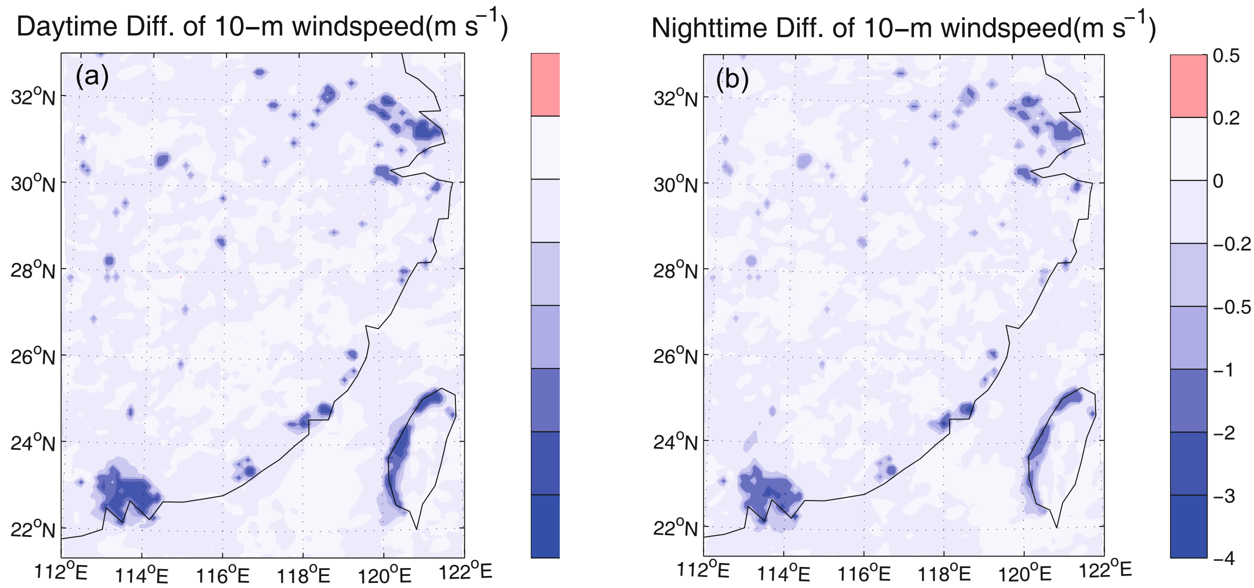

Fig. 4. As in Fig. 3, but for the difference of the monthly-averaged 10-m wind speeds.

and 1.4°C during the nighttime over urban areas. Although warm centers dominate, there are some cool centers (minimum temperature difference < -0.2°C) in the Pearl River estuary with urban expansion. Compared to the YRD, the PRD has a smaller increase of the 2-m temperatures, especially at nighttime, which can be seen in Table 2.

Urbanization decreases both daytime and nighttime 10-m wind speeds in the urban areas as shown in Fig. 4, because of rougher urban surfaces. Daytime reduction in the wind speed (more than 3 m s^{-1}) is larger than that for the nighttime (0.5 to 2 m s^{-1}). The PRD has a much larger decrease of the 10-m wind speed than the YRD at nighttime, about a 2–3 m s^{-1} decrease because the PRD cities are close to each other while the YRD cities are sparse. That means the more centralized urbanization in the PRD may lead to a larger decrease of the near-surface wind speeds.

The spatial difference of the monthly mean PBL height in the daytime and nighttime are shown in Fig. 5. Urbanization also increases both the daytime and nighttime boundary layer depth, as expected. The

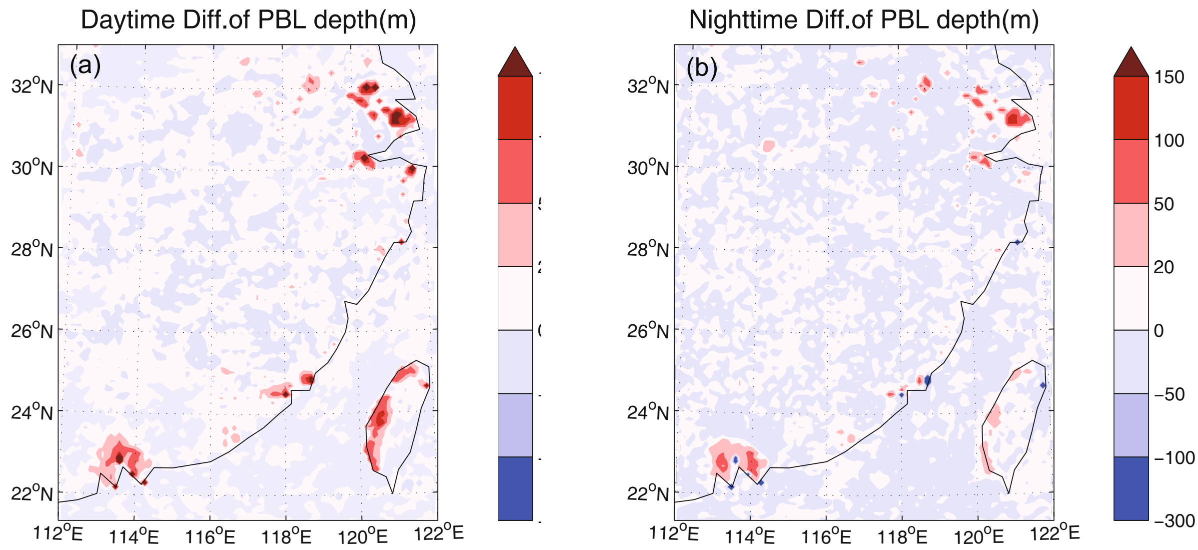

Fig. 5. As in Fig. 4, but for the differences of the monthly-averaged boundary layer depths (m).

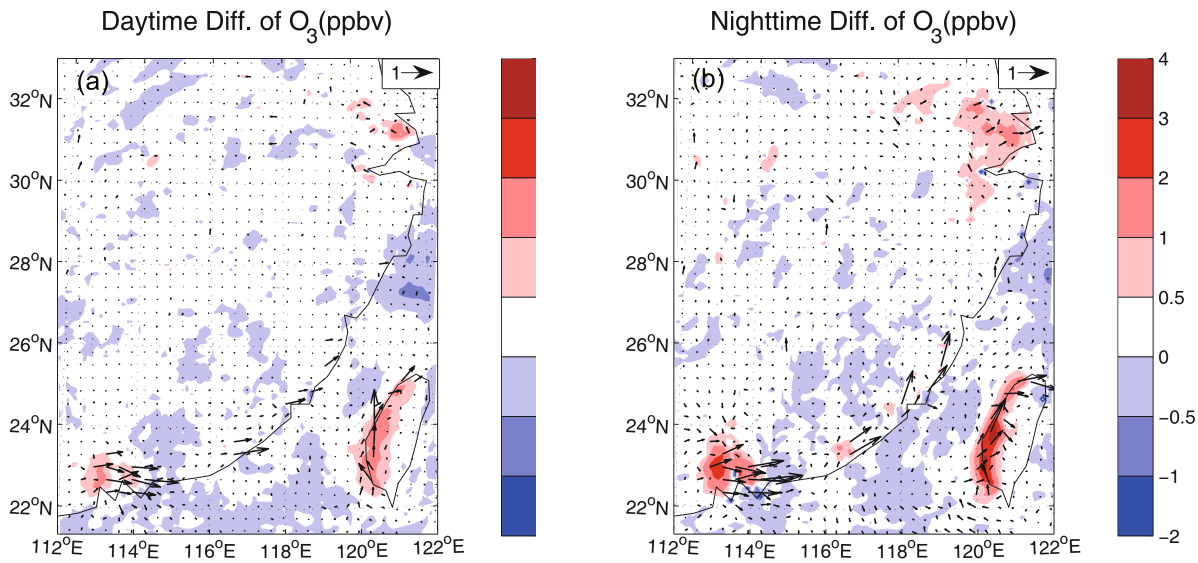

Fig. 6. Difference of the surface ozone and relative 10-m wind vectors. (a) Daytime, (b) Nighttime.

daytime increase in the PBL height (200 m) is larger than that for the nighttime (50–100 m). Moreover, the PRD has a smaller increase in the PBL depth than the YRD. During the nighttime, the PBL depth increases 35.3% in the YRD, while there is only a 5.9% increase in the PRD.

4.2 *Impact of urban expansion on surface* O_3 *concentrations*

We have seen so far that urbanization can modify temperature, wind speed, and the PBL mixing-layer depth and stability. In this section, we focus on the impacts of those modified meteorological conditions on spatial and temporal distributions of ozone (O_3) concentrations, because it is the traditional indicator of photochemical smog. Figure 6 shows the influences of urban expansion on daytime and nighttime averaged surface O_3 concentrations and the 10-m wind vector. While surface O_3 concentrations over major cities for the daytime and nighttime increase, the nighttime enhancements in O_3 concentrations outpace those during the daytime in the urban expansion regions. Areas with the main O_3 concentration increases generally coincide with the areas of temperature increases and wind speed reductions. These results are consistent with previous studies showing the direct link between increased ozone concentrations and higher temperatures (Sillman and Samson, 1995; Aw and Kleeman, 2003). Nevertheless, it should be noted that, in the daytime, the surface ozone increase (by 2.9%–4.2%) is less than that for the nighttime (about 4.7%–8.5%). This study confirms the finding of Wang et al. (2007) that the temperature enhancement and the wind speed decrease alone are not sufficient to explain changes in the surface O_3 concentrations, and the PBL-depth change plays a very important role in surface ozone concentration. At the same time, we found urbanization increases converging over the urban areas, especially in the PRD. In addition to a shallower mixing layer, the nighttime enhancement of the convergence zones is larger than that of the daytime. A smaller increase in the mixing layer and stronger convergence zones in the PRD favor both a daytime and nighttime accumulation of surface ozone.

5. Summary

In this study, we used the online chemistry model, the WRF-Chem, to conduct a month-long simulation to investigate the effects of urban expansion on surface meteorology and ozone concentrations in two rapidly-expanded urban areas located in slightly different climate regimes: PRD and YRD regions. Simulation results indicate that urbanization: (1) increases both day- and night-time 2-m temperatures by about 0.6°C and 1.4°C, respectively; (2) decreases both day- and night-time 10-m wind speeds, and the daytime reduction (by 3.0 m s^{-1}) in wind speed is larger than that for the nighttime (by 0.5 to 2 m s^{-1}); and (3) increases both day- and night-time boundary-layer depths, and the daytime increase in the PBL height (more than 200 m) is larger than that for the nighttime (50–100 m). Changes in meteorological conditions can result in detectable ozone concentration changes in the PRD and the YRD. Urbanization increases surface ozone concentrations by about 4.7%–8.5% for the nighttime and by about 2.9%–4.2% for the daytime. More importantly, despite the fact that both the PRD and the YRD have similar degrees of urbanization in the last decade and both are located in coastal zones, urbanization has different effects on the surface ozone for the PRD and the YRD, presumably due to their urbanization characteristics and geographical locations. Even though the PRD has a smaller increase in surface temperatures than the YRD, it has (a) weaker surface wind speeds, (b) a smaller increase in PBL heights, and (c) stronger convergence zones. We found that the latter three factors outweighed the temperature increase and resulted in larger ozone enhancements in the PRD than the YRD. It is worth seeing that this study reports some preliminary results, and future work will be conducted to understand the impact of emission changes accompanied with land-use and land-cover changes.

Acknowledgements. The work described in this paper was supported by the National Natural Science Foundation of China (Grant Nos. 40875076, U0833001, and 40645024) and the National Center for Atmospheric Research (NCAR) FY07 Director Opportunity Fund. This work also supported by the Knowledge Innovation Program of the Chinese Academy of Sciences (IAP 07306), the Institute of Atmospheric Physics, the Chinese Academy of Sciences(LAPC-KF-2006-12), the Scientific Research Foundation for the Returned Overseas Chinese Scholars, State Education Ministry of China.

REFERENCES

Aw, J., and M. Kleeman, 2003: Evaluating the first-order effect of intraannual temperature variability on urban air pollution. *J. Geophys. Res.*, **108**(D12), 4365, doi: 10.1029/2002JD002688.

Bey, I., D. J. Jacob, J. A. Logan, and R. M. Yantosca, 2001: Asian chemical outflow to the Pacific in spring: Origins, pathways and budgets. *J. Geophys. Res.*, **106**, 23097–23113.

Carmichael, G. R., and Coauthors, 2003a: Evaluating regional emission estimates using the TRACE-P observations. *J. Geophys. Res.*, **108**(D21), 8810, doi: 10.1029/2002JD003116.

Carmichael, G. R., and Coauthors, 2003b: Regional-scale chemical transport modeling in support of intensive field experiments: Overview and analysis of the TRACE-P observations. *J. Geophys. Res.*, **108**(D21), 8823, doi: 10.1029/2002JD003117.

Chan, C. Y., L. Y. Chan, H. Cui, X. D. Zheng, Y. G. Zheng, Y. Qin, and Y. S. Li, 2003: Origin of the springtime tropospheric ozone maximum over east China at LinAn in 2001. *Tellus*, **55B**, 982–992.

Chan, L. Y., H. Y. Liu, , K. S. Lam, T. Wang, S. J. Oltmans, and J. M. Harris, 1998: Analysis of the seasonal behavior of tropospheric ozone at Hong Kong. *Atmos. Environ.*, **32**, 159–168.

Charney, J., W. J. Quirk, S. H. Chow, and J. Kornfield, 1977: A comparative study of the effects of albedo change on drought in semi-arid regions. *J. Atmos. Sci.*, **34**, 1366–1385.

Chase, T. N., R. A. Pielke, T. G. F. Kittel, R. Nemani, and S. W. Running, 1996: The sensitivity of a general circulation model to large-scale vegetation changes. *J. Geophys. Res.*, **101**, 7393–7408.

Chen, F., and J. Dudhia, 2001: Coupling and advanced land surface-hydrology model with the Penn State-NCAR MM5 modeling system. Part I: Model implementation and sensitivity. *Mon. Wea. Rev.*, **129**, 569–585.

Civerolo, K. L., G. Sistla, S. T. Rao, and D. J. Nowak, 2000: The effects of land use in meteorological modeling: Implications for assessment of future air quality scenarios. *Atmos. Environ.*, **34**(10), 1615–1621.

Civerolo, K. L., and Coauthors, 2007: Estimating the effects of increased urbanization on surface meteorology and ozone concentrations in the New York City metropolitan region. *Atmos. Environ.*, **41**, 1803–1818.

Dudhia, J., 1989: Numerical study of convection observed during the winter monsoon experiment using a mesoscale two dimensional model. *J. Atmos. Sci.*, **46**, 3077–3107.

Fast, J. D., and Coauthors, 2006: Evolution of ozone, particulates, and aerosol direct radiative forcing in the vicinity of Houston using a fully coupled meteorology-chemistry aerosol model. *J. Geophys. Res.*, **111**(D21305), doi: 10.1029/2005JD006721.

Fishman, J., and V. G. Brackett, 1997: The climatological distribution of tropospheric ozone derived from satellite measurements using version 7 Total Ozone Mapping Spectrometer and Stratospheric Aerosol and Gas Experiment data sets. *J. Geophys. Res.*, **102**(D15), 19275–19278.

Foley, J. A., and Coauthors, 2005: Global consequences of land use: Review. *Science*, **309**, 570–574.

Friedl, M. A., D. K. McIver, and J. C. F. Hodges, 2002: Global land cover mapping from MODIS: Algorithms and early results. *Remote Sens. Environ.*, **83**, 287–302.

Grell, G., and Coauthors, 2005: Fully coupled "online" chemistry within the WRF model. *Atmos. Environ.*, **39**, 6957–6975.

Grossman-Clarke, S., J. A. Zehnder, W. L. Stefanov, Y. Liu, and M. A. Zoldak, 2005: Urban modifications in a mesoscale meteorological model and the effects on near-surface variables in an arid metropolitan region. *J. Appl. Meteor.*, **44**, 1281–1297.

Guenther, A., and Coauthors, 1995: A global-model of natural volatile organic-compound emissions. *J. Geophys. Res.*, **100**(D5), 8873–8892.

Harris, J. M., S. J. Oltmans, E. J. Diugokencky, P. C. Novelli, B. J. Johnson, and T. Mefford, 1998: An investigation into the source of the springtime tropospheric ozone maximum at Mauna Loa Observatory. *Geophys. Res. Lett.*, **25**, 1895–1898.

He, J. F., and D. F. Zhuang, 2005: Analyses the relationship between urban dynamic change pattern of the Yangtze River Delta and the ecological environment. *IEEE CNF*, **1**, 245–248.

Hong, S.-Y., H.-M. H. Juang, and Q. Zhao, 1998: Implementation of prognostic cloud scheme for a regional spectral model. *Mon. Wea. Rev.*, **126**, 2621–2639.

Inoue, E., 1963: On the turbulent structure of air flow within crop canopies, *J. Meteor. Soc. Japan*, **41**(6), 317–326.

Jiang, X., C. Wiedinmyer, F. Chen, Z.-L. Yang, and J. C.-F. Lo, 2008: Predicted impacts of climate and land use change on surface ozone in the Houston, Texas, area. *J. Geophys. Res.*, **113**, D20312, doi: 10.1029/2008JD009820.

Kain, J. S., 2004: The Kain-Fritsch convective parameterization: An update. *J. Appl. Meteor.*, **43**, 170–181.

Kusaka, H., and F. Kimura, 2004: Coupling a single-layer urban canopy model with a simple atmospheric model: Impact on urban heat island simulation for an idealized case. *J. Meteor. Soc. Japan*, **82**, 67–80.

Kusaka, H., H. Kondo, Y. Kikegawa, and F. Kimura, 2001: A simple single-layer urban canopy model for atmospheric models: Comparison with multi-layer and slab models. *Bound.-Layer Meteor.*, **101**, 329–358.

Langford, A. O., 1999: Stratosphere-troposphere exchange at the subtropical jet contribution to the tropospheric ozone budget at midlatitudes. *Geophys. Res. Lett.*, **26**, 2449–2452.

Lee, Y. L., and R. Sequeira, 2001: Visibility degradation across Hong Kong: Its components and their relative contributions. *Atmos. Environ.*, **34**, 5861–5872.

Liang, J. Y., and S. S. Wu, 1999: Climatological diagnosis of winter temperature variations in Guangdong. *Journal of Tropical Meteorology*, **15**(3), 221–229. (in Chinese)

Lin, W. S., and Coauthors, 2007: A numerical study of the influence of urban expansion on monthly climate in dry autumn over Pearl River Delta, China. *Theor. Appl. Climatol.*, **89**(1–2), 63–72.

Liu, Y., F. Chen, T. Warner, and J. Basara. 2006: Verification of a mesoscale data-assimilation and forecasting system for the Oklahoma city area during the Joint Urban 2003 Field Project. *Journal of Applied Meteorology*, **45**, 912–929.

Lo, J., A. Lau, J. Fung, and F. Chen, 2006: Role of land-sea-breeze circulations modified by urbanization on air pollution in the Pearl River Delta Region. *J. Geophys. Res.*, **111**, D14104, doi: 10.1029/2005JD006837.

Logan, J. A., 1985: Tropospheric ozone: Seasonal behavior, trends, and anthropogenic influence. *J. Geophys. Res.*, **90**, 463–482.

Miao, S., and F. Chen, 2008: Formation of horizontal convective rolls in urban areas. *Atmospheric Research*, **89**, 298–304.

Miao, S., F. Chen, M. A. LeMone, M. Tewari, Q. Li, and Y. Wang, 2009: An observational and modeling study of characteristics of urban heat island and boundary layer structures in Beijing. *Journal of Applied Meteorology*, **48**, 484–501.

Mlawer, E. J., S. J. Taubman, P. D. Brown, M. J. Iacono, and S. A. Clough, 1997: Radiative transfer for inhomogeneous atmospheres: RRTM, a validated correlated-k model for the longwave. *J. Geophys. Res.*, **102**, 16663–16682.

Noh, Y., W. G. Cheon, S.-Y. Hong, and S. Raasch, 2003: Improvement of the Kprofile model for the planetary boundary layer based on large eddy simulation data. *Bound.-Layer Meteor.*, **107**, 401–427.

Oltmans, S. J., and H. II. Levy, 1992: Seasonal cycle of surface ozone over the western north Atlantic. *Nature*, **358**, 392–394.

Ordonez, C., H. Methis, M. Furger, S. Henne, C. Huglin,

J. Staehelin, and A. S. H. Prevot, 2005: Changes of daily surface ozone maxima in Switzerland in all seasons from 1992 to 2002 and discussion of summer 2003. *Atmospheric Chemistry and Physics*, **5**, 1187–1203.

Schlünzen, K. H., and J. J. Katzfey, 2003: Relevance of sub-grid-scale land-use effects for mesoscale models. *Tellus*, **55A**, 232–246.

Sillman, S., and P. J. Samson, 1995: Impact of temperature on oxidant photochemistry in urban, polluted rural and remote environments. *J. Geophys. Res.*, **100**, 11497–11508.

Streets, D. G., and Coauthors, 2003: A year-2000 inventory of gaseous and primary aerosol emissions in Asia to support TRACE-P modeling and analysis. *J. Geophys. Res.*, **108**(D21), 8809, doi: 10.1029/2002JD003093.

Taha, H., S. Konopacki, and H. Akbari, 1998: Impacts of lowered urban air temperatures on precursor emission and ozone air quality. *Journal of the Air and Waste Management Association*, **48**, 860–865.

Wang, T., Y. Y. Wu, T. F. Cheung, and K. S. Lam, 2001: A study of surface ozone and the relation to complex wind flow in Hong Kong. *Atmos. Environ.*, **35**, 3203–3215.

Wang, T., A. J. Ding, D. R. Blake, W. Zahorowski, C.N. Poon, and Y. S. Li, 2003a: Chemical characterization of the boundary layer outflow of air pollution to Hong Kong during February–April 2001. *J. Geophys. Res.*, **108**(D20), 8787.

Wang, T., C. N. Poon, Y. H. Kwok, and Y. S. Li, 2003b: Characterizing the temporal variability and emission patterns of pollution plumes in the Pearl River Delta of China. *Atmos. Environ.*, **37**, 3539–3550.

Wang, X. M., G. R. Carmichael, D. L. Chen, and Y. H. Tang, 2005: Impacts of different emission sources on air quality during March 2001 in the Pearl River Delta (PRD) region. *Atmos. Environ.*, **39**(29), 5227–5241.

Wang, X. M., W. S. Lin, L. M. Yang, R. R. Deng, and H. Lin, 2007: A numerical study of influences of urban land-use change on ozone distribution over the Pearl River Delta Region, China. *Tellus*, **59B**, 633–641.

Wild, O., X. Zhu, and M. J. Prather, 2000: Fast-J: Accurate simulation of in- and below cloud photolysis in tropospheric chemical models. *Journal of Atmospheric Chemistry*, **37**, 245–282.

Yao, S. M., and S. Chen, 1998: Urban sprawl in spatial tendency in Yangtze River delta region. *Chinese Journal of Geographical Sciences*, **53**(6), 10–15.

Zaveri, R. A., and L. K. Peters, 1999: A new lumped structure photochemical mechanism for large-scale applications. *J. Geophys. Res.*, **104**, 30387–30415.